

Article

# A Homogeneous Colorimetric Strategy Based on Rose-like CuS@Prussian Blue/Pt for Detection of Dopamine

Di Yang, Jiao Ran, Huafei Yi, Pujin Feng and Bingqian Liu \* 

Guizhou Engineering Laboratory for Synthetic Drugs (Ministry of Education of Guizhou Province),  
College of Pharmacy, Guizhou University, Guiyang 550025, China

\* Correspondence: nqliu@gzu.edu.cn

**Abstract:** The development of effective methods for dopamine detection is critical. In this study, a homogeneous colorimetric strategy for the detection of dopamine based on a copper sulfide and Prussian blue/platinum (CuS@PB/Pt) composite was developed. A rose-like CuS@PB/Pt composite was synthesized for the first time, and it was discovered that when hydrogen peroxide was present, the 3,3',5,5'-tetramethylbenzidine (TMB) changed from colorless into blue-oxidized TMB. The CuS@PB/Pt composite was characterized with a scanning electron microscope (SEM), an energy dispersive spectrometer (EDS), and an X-ray photoelectron spectrometer (XPS). Moreover, the catalytic activity of the CuS@PB/Pt composite was inhibited by the binding of dopamine to the composite. The color change of TMB can be evaluated by the UV spectrum and a portable smartphone detection device. The developed colorimetric sensor can be used to quantitatively analyze dopamine between 1 and 60  $\mu\text{M}$  with a detection limit of 0.28  $\mu\text{M}$ . Furthermore, the sensor showed good long-term stability and good performance in human serum samples. Compared with other reported methods, this strategy can be performed rapidly (16 min) and has the advantage of smartphone visual detection. The portable smartphone detection device is portable and user-friendly, providing convenient colorimetric analysis for serum. This colorimetric strategy also has considerable potential for the development of in vitro diagnosis methods in combination with other test strips.

**Keywords:** colorimetric; dopamine; rose-like CuS@Prussian blue/Pt; smartphone



**Citation:** Yang, D.; Ran, J.; Yi, H.; Feng, P.; Liu, B. A Homogeneous Colorimetric Strategy Based on Rose-like CuS@Prussian Blue/Pt for Detection of Dopamine. *Sensors* **2023**, *23*, 9029. <https://doi.org/10.3390/s23229029>

Academic Editors: Fengqing Yang and Liya Ge

Received: 22 August 2023

Revised: 27 October 2023

Accepted: 31 October 2023

Published: 7 November 2023



**Copyright:** © 2023 by the authors. Licensee MDPI, Basel, Switzerland. This article is an open access article distributed under the terms and conditions of the Creative Commons Attribution (CC BY) license (<https://creativecommons.org/licenses/by/4.0/>).

## 1. Introduction

Dopamine (DA) is an important neurotransmitter that plays a key role in neuropsychiatric illness [1]. DA is an important and abundant monoamine neurotransmitter that is closely connected to many neuronal activities, such as cognitive function [2], motor control [3], and memory function [4]. In particular, the pathophysiology of several psychiatric and neurological conditions, including Parkinson's disease [3], Huntington's disease [5], food and drug addiction [6], and schizophrenia [7], is intimately linked to aberrant DA secretion. Parkinson's disease is the second most common neurodegenerative disease; however, the early pathophysiological events and sequences of its dysfunction remain unknown. The loss of dopaminergic neurons and lower levels of striatal DA can lead to the motor impairments in Parkinson's disease [3]. Therefore, the development of an efficient, consistent, and sensitive method of detecting DA is crucial.

Recently, several techniques have been developed for DA detection, including high-performance liquid chromatography (HPLC) [8], liquid chromatography-mass spectrometry (LC-MS) [9], electrochemical methods [10–12], fluorescence spectrophotometry [13], and colorimetric sensors [14]. These methods have demonstrated advantages in terms of accuracy and precision. However, these methods, more or less, have some weaknesses. For example, the HPLC and LC-MS have disadvantages such as time consumption, expensive instruments, and operator training. Electrochemical detection has been widely noticed because of its low cost, fast detection, high sensitivity, and simple operation, but it is

relatively less intuitive. The colorimetric assay has the advantages of simplicity, rapidity, and intuitiveness. It has also been reported that an electrochemical-colorimetric dual-mode detection of dopamine has been established [14]. Moreover, there have also been reports of colorimetric detection using smartphones by capturing the color changes without the need for additional tools. Colorimetric sensors are based on enzymes that change their color and absorbance during DA detection. Since these sensors are inexpensive, portable, rapid-acting, and clearly visible to the naked eye, they have been extensively utilized for DA detection [15–17].

Nowadays, many nanomaterials are known to exhibit enzyme-like activity. These nanomaterials include precious metal nanoparticles [18], metal oxides [19], metal sulfides, carbon nanotubes [20], graphene and derivatives [21], metal-organic frameworks [22], etc. Recently, precious metal nanomaterials such as platinum nanoparticles (NPs) have been considered promising candidates for application in colorimetric sensors owing to their peroxidase activity [23]. However, they regularly group together in catalytic reactions, which decreases the catalytic activity. Currently, an efficient solution to this issue is the hybrid nanomaterials created by growing Pt NPs on substrates such as graphene oxide, MoS<sub>2</sub> nanosheets, MoO<sub>3</sub> nanosheets, and Pd nanosheets [24–27]. More importantly, these hybrid nanomaterials' catalytic activity can be significantly increased due to the synergistic interaction between their bimetallic active centers. Cu-based nanomaterials such as copper oxide (CuO) [28] and copper phosphate Cu<sub>3</sub>(PO<sub>4</sub>)<sub>2</sub> [29] have received a great deal of attention for sensing and catalysis-related applications [30]. Due to their enzymatic-like behavior for the catalyzed oxidation of per-oxidase substrates in the presence of H<sub>2</sub>O<sub>2</sub>, copper sulfide (CuS)-based nanomaterials have been shown to be promising nanozymes for glucose, cholesterol, and uric acid sensing [31]. A CuS-based sensor for sensing dopamine has previously been reported in conjunction with rGO [32]. Among them, Prussian blue (PB) has attracted a lot of study interest because of its significant peroxidase mimic catalytic activity, which is related to its mixed valence states of Fe atoms, which are similar to Fe<sub>3</sub>O<sub>4</sub> [33,34]. Due to their excellent peroxidase mimic characteristics, they are commonly employed as transducers in the development of electrochemical biosensors [34]. Prussian blue (PB) NPs with high enzyme-mimicking activity supported by MoS<sub>2</sub> nanocomposites have been reported as peroxidase-like nanozymes for the colorimetric sensing of DA [35–37]. Compared with single nanomaterials, multi-component systems may be able to solve the above problems and can generally exhibit high enzymatic simulation catalytic activity.

In this study, we developed a rapid, homogeneous colorimetric method based on copper sulfide Prussian blue/platinum (CuS@PB/Pt) NP composites for DA detection. The colorimetric performance of the NPs was improved by the addition of Pt. To effectively replace natural enzymes like horseradish peroxidase (HRP) in the chromogenic reaction between H<sub>2</sub>O<sub>2</sub> and 3,3',5,5'-tetramethylbenzidine (TMB), the CuS@PB/Pt NP composites were synthesized. DA successfully prevented the chromogenic reaction by oxidizing colorless TMB to blue oxidized TMB (ox-TMB), effectively turning off the colorimetric signals. This assay was validated for the detection of DA in human serum. This method provides a strategy for DA identification and may be suitable for practical application.

## 2. Materials and Methods

### 2.1. Reagents and Apparatus

The details are described in the Supplementary Materials.

### 2.2. Synthesis of CuS@PB/Pt

The CuS NPs and CuS@PB composites were prepared using methods described by Qu et al. [38] and Li et al. [39], whereas the CuS@PB/Pt composite was prepared using a method described by Gong et al. [28]. The Supplementary Materials contain a detailed description of the preparation procedures.

### 2.3. Colorimetric Detection of DA

In PBS buffer (0.01 M, pH = 7, 320  $\mu$ L), different concentrations of DA aqueous solution were mixed with CuS@PB/Pt (1 mg/mL, 30  $\mu$ L). Then, TMB (50 mM dissolved in ultrapure water, 110  $\mu$ L) and H<sub>2</sub>O<sub>2</sub> (50 mM, 50  $\mu$ L) were added to the above solution. After 16 min of incubation at 45 °C, the mixture was subjected to UV-vis absorption spectroscopy to measure the absorbance. A calibration curve was prepared by plotting the absorbance at 652 nm as a function of the DA concentration ( $A = A_0 - A$ , where  $A_0$  and  $A$  are the absorbance values at 652 nm in the absence and presence of DA, respectively). We took pictures immediately, and the RGB value of the color change of the reaction system was extracted using the built-in chromaticity extraction software (Color extractor, Android app market). The  $R$  value was used to quantitatively determine the DA concentration in the system. A portable smartphone colorimetric detection device was developed according to the method reported by Qu et al. [40]. We made a slight improvement by adding a cover to the device to avoid affecting the stability of the method due to a change in the light source. A schematic of the device is shown in Figure 1c.

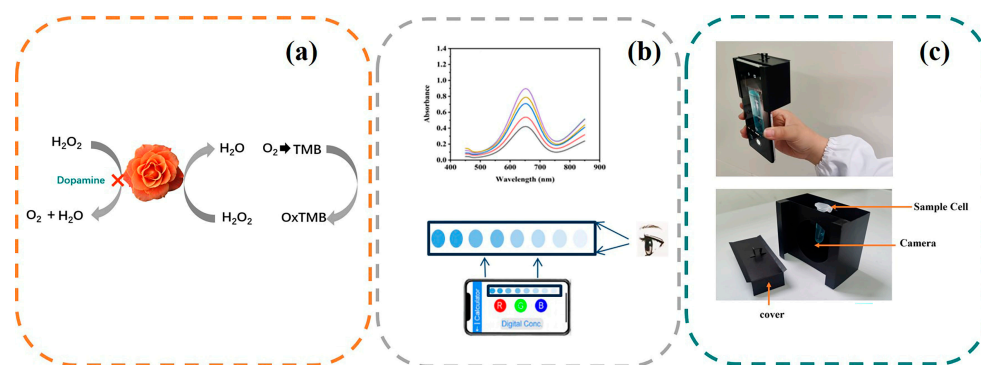


**Figure 1.** (a) Schematic illustration of a CuS@Pb/Pt colorimetric sensor for DA. (b) Two methods for detecting dopamine. (Coloured lines for UV-vis absorption spectroscopy; Shades of blue for visible color of DA) (c) The schematic representation of the portable device.

### 2.4. Quantitative Analysis of DA in Human Serum Samples

To successfully detect DA in human serum, samples from healthy volunteers were obtained from the Guizhou Staff Hospital (Guizhou, China). Before use and after thawing at room temperature, the samples were centrifuged (6708  $\times$  g) for 10 min to precipitate macromolecular proteins and other impurities, and the supernatant was diluted 50 $\times$  for testing. In addition, different concentrations of DA standard solution (2–30 ng/mL) were added to the prepared serum samples and measured using UV-vis absorption spectroscopy and a smartphone. The recovery rate was calculated using the following formula:

$$\text{Recovery}(\%) = \frac{C_{\text{detected}} - C_{\text{added}}}{C_{\text{added}}} \times 100\% \quad (1)$$

## 3. Results

### 3.1. Characterization of Materials

To ensure the success of the experiment, it was important to determine whether the CuS@PB/Pt composite had been properly synthesized. First, the morphologies of CuS, CuS@PB, and CuS@PB/Pt were characterized using SEM. As shown in Figure 2a, the CuS NPs exhibited the shape of a rose composed of nanosheets. The thickness of the nanosheets was uniform and clear [38]. The CuS@PB (Figure 2b) changes in morphology mean that the thickness of the nanosheets was thicker. As shown in Figure 2c, the CuS@PB/Pt composite recovered its flower shape, and small particles were present on the nanosheets. In addition, the EDS results revealed the presence of S, Fe, Cu, and Pt in the CuS@PB/Pt composite (Figure 2d,h,i).

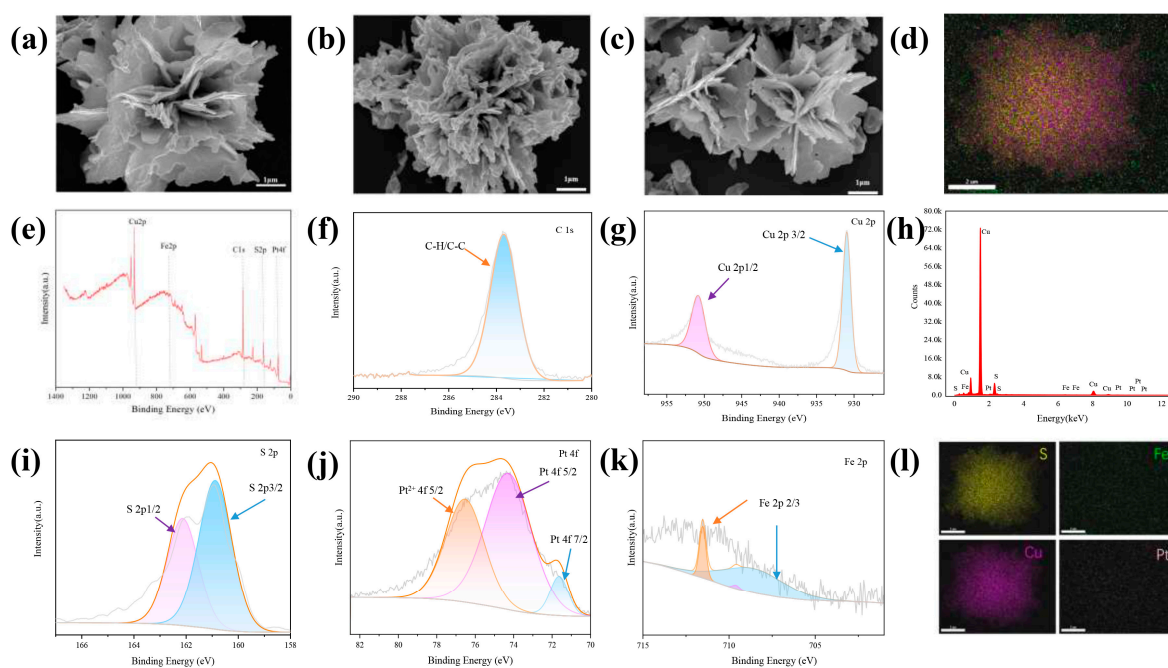


**Figure 2.** SEM images of (a) CuS, (b) CuS@PB, and (c) CuS@PB/Pt. (e) XPS spectra of the CuS@PB/Pt. XPS spectra of (f) C 1s, (g) Cu 2p, (i) S 2p, (j) Pt 4f, and (k) Fe 2p. (d,h,l) The corresponding EDS elemental mapping images of the prepared CuS@PB/Pt, including the S, Cu, Fe, and Pt. Scale bar: 2 nm.

X-ray photoelectron spectroscopy (XPS) was used to further investigate the chemical composition of the CuS@PB/Pt composites. As shown in Figure 2g, there were two main characteristic peaks at 930.97 and 950.78 eV in the Cu2p spectrum, which were assigned to Cu 2p<sub>3/2</sub> and Cu 2p<sub>1/2</sub>, respectively. Peaks corresponding to S 2p appeared at 160.88 eV (S 2p<sub>3/2</sub>) and 162.13 eV (S 2p<sub>1/2</sub>) [39] (Figure 2i). The Pt 4f profile showed two peaks at 71.63 and 76.53 eV, which correspond to metallic Pt 4f<sub>7/2</sub> and Pt 4f<sub>5/2</sub>, respectively. Pt mainly exists in the zero-valence and 2<sup>+</sup>-valence forms. Three peaks in the Fe 2p spectrum (Figure 2k), which correspond to Fe 2p<sub>3/2</sub>, are evident at approximately 708.6, 709.6, and 711.53 eV [39].

### 3.2. Feasibility of the Designed Colorimetric Strategy

Evaluation of the oxidase activity of the CuS@PB/Pt composite is essential because it directly influences the TMB signal response. First, we studied the oxidase activity of the synthesized materials using UV-vis absorption spectroscopy. TMB, the most widely used chromogenic substrate in nanoenzyme catalysis, was used as a chromogenic reagent in this experiment. Typically, CuS@PB/Pt (1 mg/mL, 30  $\mu$ L) was dispersed into PBS buffer (0.01 M, pH = 7, 320  $\mu$ L) and ultrapure water (480  $\mu$ L). TMB (50 mM, 110  $\mu$ L) and H<sub>2</sub>O<sub>2</sub> (50 mM, 50  $\mu$ L) were added to the solution. The TMB was dissolved in ultrapure water. The mixture was incubated at 37  $^{\circ}$ C for 10 min. After that, the absorbance data were immediately collected using UV-vis absorption spectroscopy. The peroxidase-like catalytic activities of CuS, CuS@PB, and CuS@PB/Pt (1.0 mg/mL) were investigated. As shown in Figure 3a, the CuS@PB/Pt composites exhibited a high absorbance of 652 nm compared to the other components, such as CuS and CuS@PB. Moreover, except when H<sub>2</sub>O<sub>2</sub> and the CuS@PB/Pt composite existed at the same time, the absence of an absorption peak at 652 nm in the other components further demonstrates the superiority of the composite over the alternatives (Figure 3b). This phenomenon agrees with previous reports that H<sub>2</sub>O<sub>2</sub> would first be quickly catalyzed into hydroxyl radicals in the presence of peroxidase, which would then further oxidize the colorless TMB to a blue ox-TMB [41].

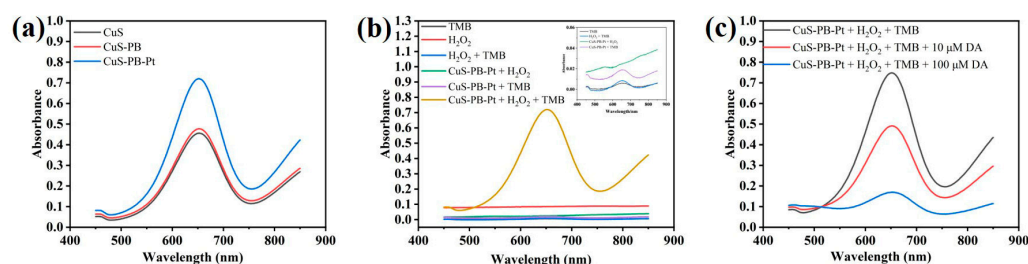


**Figure 3.** (a) Responses of UV-vis spectra of various materials to TMB and  $H_2O_2$  at the same concentration (1.0 mg/mL). (b) Responses of the UV-vis spectra of CuS@PB/Pt (1.0 mg/mL) reacted with TMB with or without  $H_2O_2$ . (c) Responses of UV-vis spectra to the addition of DA at different concentrations.

In addition, we investigated the oxidase activity of the CuS@PB/Pt composite using a color-producing process. The CuS@PB/Pt composite oxidized colorless TMB to blue ox-TMB in the presence of hydrogen peroxide. The oxidative activity was demonstrated by Michaelis–Menten kinetics ( $v = V_{max}[S]/(K_m + [S])$ ), where  $[S]$  is the concentration of the substrate,  $v$  is the initial velocity,  $K_m$  is the Michaelis–Menten constant, and  $V_{max}$  is the maximal reaction velocity.

As shown in Figure S1a,c, CuS@PB/Pt had a  $K_m$  value of 3.5 mM when  $H_2O_2$  was used as the substrate, which was less than that previously observed for HRP (3.70 mM) [42]. Unlike HRP, which has a  $K_m$  value of 0.434 mM, the CuS@PB/Pt nanocomposites have a  $K_m$  value of 0.298 mM (Figure S1b,d) with TMB as the substrate. In addition, the feasibility of the proposed colorimetric strategy for the detection of DA was explored. As shown in Figure 3c, when DA was added in various quantities, the ox-TMB absorption peak at 652 nm decreased in intensity (10  $\mu$ M, 100  $\mu$ M). To further investigate the feasibility of the suggested colorimetric strategy, the oxidative reactions of other chromogenic reagents such as 2,2'-azino-bis(3-ethylbenzothiazoline-6-sulfonic acid) (ABTS) and *o*-phenylenediamine (OPD) were also performed (Figure S3a,b). The characteristic absorbance of the UV-vis spectra (Figure S2a,b) indicates that the colorimetric strategy for DA detection was successfully developed.

### 3.3. Optimization of Experimental Parameters

HRP and other peroxidase mimics are comparable to natural peroxidases, and the pH and temperature of the experiment can significantly impact the catalytic ability of the CuS@PB/Pt composites. To investigate how pH affects the catalytic oxidation of TMB by CuS@PB/Pt in the presence of  $H_2O_2$ , we conducted pH experiments using buffer solutions with different pH values. In Figure 4a, the changes in the peroxidase-like activity of the CuS@PB/Pt composites are shown at different pH levels (3.0–8.0). The findings show that the best catalytic activity was achieved at approximately pH 7. Therefore, a pH of 7 was selected for the ensuing test. Additionally, a broad temperature range (20–60  $^{\circ}$ C) was examined to find out how temperature affected the catalytic activity of CuS@PB/Pt. The catalytic activity of CuS@PB/Pt was found to be at its optimum level at 45  $^{\circ}$ C (see Figure 4b). These results are consistent with those of Figure 3d, which suggests that the relative activity of CuS@PB/Pt is maintained above 40% over the temperature range of 20  $^{\circ}$ C to 60  $^{\circ}$ C. The response time of the CuS@PB/Pt composite to ox-TMB was also investigated. When the CuS@PB/Pt composites interacted with TMB, the UV-vis spectra of ox-TMB tended to be maximal and constant after 16 min of reaction, as shown in Figure 4c.

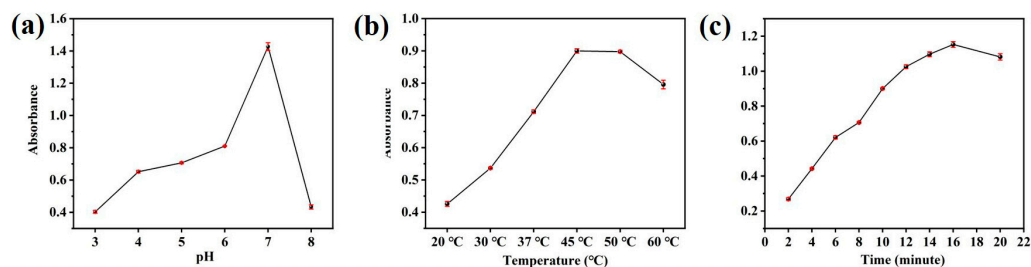


**Figure 4.** (a) UV-vis absorption spectra with different pHs of PBS (0.01 M) buffer. (b) UV-vis absorption spectra with different reaction temperatures. (c) UV-vis absorption spectra with different reaction times.

### 3.4. Analytical Performance of Colorimetric Detection of DA

To evaluate the sensing capacity of CuS@PB/Pt for the colorimetric detection of DA, various concentrations (1–60  $\mu\text{M}$ ) of DA were measured under the optimal conditions. As shown in Figure 5a, the absorbance decreased progressively as the DA content increased, which is compatible with the color change shown in Figure 5c. There were two linear ranges at low (1–10  $\mu\text{M}$ ) and high concentrations (10–60  $\mu\text{M}$ ) of DA. The following regression equation applies:  $y_1 = -0.031x_1 + 1.1195$  ( $R^2 = 0.993$ ), where  $x_1$  is the concentration of 1–10  $\mu\text{M}$ ;  $y_2 = -0.011x_2 + 1.119$  ( $R^2 = 0.993$ ), where  $x_2$  is the concentration of 10–60  $\mu\text{M}$ , and the detection limit is 0.28  $\mu\text{M}$ . In addition, we captured the color changes on a smartphone. According to the  $R$  value produced by the smartphone, the DA concentration has a linear relationship with color at low concentrations (1–10  $\mu\text{M}$ ). The linear regression equation is as follows:  $y = 6.5182x - 0.6515$  ( $R^2 = 0.9921$ ), and 0.42  $\mu\text{M}$  is the detection limit. The linear concentration range and detection limit for DA measurement in this study are consistent with those of previous DA detection methods (Table 1). These results have the advantages of a short detection time, the use of portable equipment, and detection by smartphone.

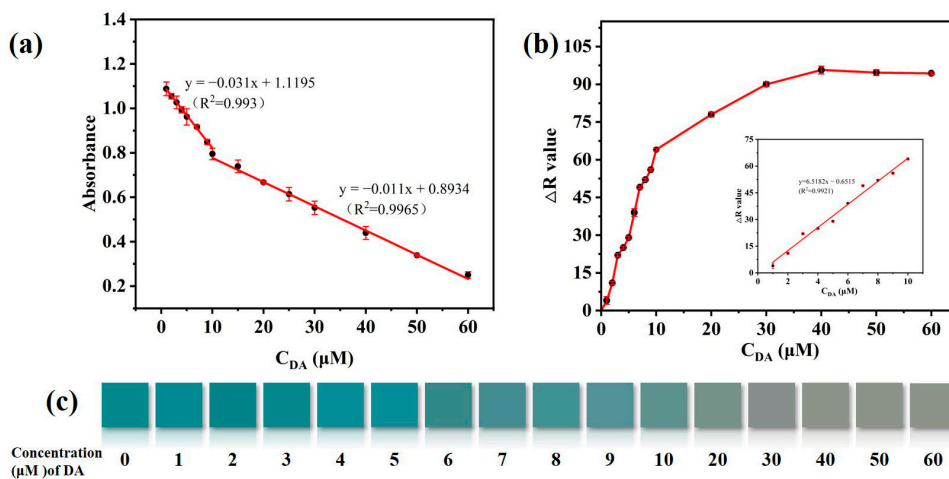


**Figure 5.** (a) Linear curve of UV-vis spectra responses in the DA from 1 to 60  $\mu\text{M}$ . (b) Linear curve of RGB colorimetry in the DA from 1 to 10  $\mu\text{M}$ . (c) Matching visible color in the DA range of 1 to 60  $\mu\text{M}$ .

**Table 1.** Comparison of different methods for the detection of dopamine.

| Method          | Materials   | LOD                | Sensitivity                               | Ref       |
|-----------------|---|--------------------|---|-----------|
| HPLC-MS/MS      | /   | 1.87 $\mu\text{M}$ | $1.87 \times 10^{-5}$ –1.87 $\mu\text{M}$ | [9]       |
| Electrochemical | $\text{Co}_3\text{O}_4$ – $\text{Fe}_2\text{O}_3$ | 0.24 $\mu\text{M}$ | 10–100 $\mu\text{M}$                      | [41]      |
| Fluorescence    | 2, 3-diaminophenazine                             | 1.76 $\mu\text{M}$ | 2.0–61 $\mu\text{M}$                      | [13]      |
| Colorimetric    | MVCM  | 0.74 $\mu\text{M}$ | 5–100 $\mu\text{M}$                       | [42]      |
| Colorimetric    | CuS@PB/Pt   | 0.28 $\mu\text{M}$ | 1–60 $\mu\text{M}$                        | This work |

### 3.5. Selectivity, Reproducibility, and Stability of the Colorimetric Method

Several common ions in human serum were studied under the same conditions to assess the selectivity of the novel colorimetric technique for DA detection. As shown in Figure 6a, only DA can drastically reduce the signal intensity. However, although their concentration was five times greater than that of DA (250  $\mu\text{M}$ ), the other ions seldom led to a discernible loss in signal intensity. As shown in Figure 6d, the same result was obtained using the smartphone to measure the  $R$  value. At the same time, Figure 6a,e shows that the absorbance of the other interferences, with the exception of AA, remains almost unchanged in the colorimetric sensor. Therefore, we introduced a masking agent, iodoacetamide (IAM), to address this issue. The introduction of IAM shields the interfering signal response well, thereby improving the selectivity of the sensor for DA, as shown in Figure 6b,f. Additionally, we evaluated the reproducibility of the suggested method using intra- and inter-batch experiments. Three different concentrations of DA (5  $\mu\text{M}$ , 10  $\mu\text{M}$ , and 30  $\mu\text{M}$ ) were tested using the same batch of synthetic CuS@PB/Pt composite. The relative standard deviation (RSD) corresponding to the absorbance values of three parallel experimental groups was less than 0.80%. The RSD values corresponding to  $R$  with three different concentrations (2  $\mu\text{M}$ , 5  $\mu\text{M}$ , and 10  $\mu\text{M}$ ) were less than 0.01%. Three batches of CuS@PB/Pt composites were used to detect DA samples (10  $\mu\text{M}$ ). The RSD values were below 1.19% and 0.8%, respectively. Additionally, under the same experimental conditions, samples prepared at the same DA concentration were tested seven times to evaluate the repeatability of this method. The UV-vis spectral responses and  $R$  values of the seven replicates were similar, indicating that the constructed sensor had satisfactory reproducibility (Figure 6b,e). This indicates that the colorimetric method has satisfactory reproducibility. We further examined the stability of the CuS@PB/Pt composite because the system had a significant impact on sample detection. When the response of the CuS@PB/Pt composite was examined after storage at 4  $^{\circ}\text{C}$  for 30 d, the absorbance of 5  $\mu\text{M}$  DA changed rarely. As shown in Figure 6f, the same result was obtained using the smartphone to determine  $R$ . This demonstrates the excellent stability of the fabricated system. The result indicates that the CuS@PB/Pt composite has the potential for use in long-term applications. to be used for long-term applications.

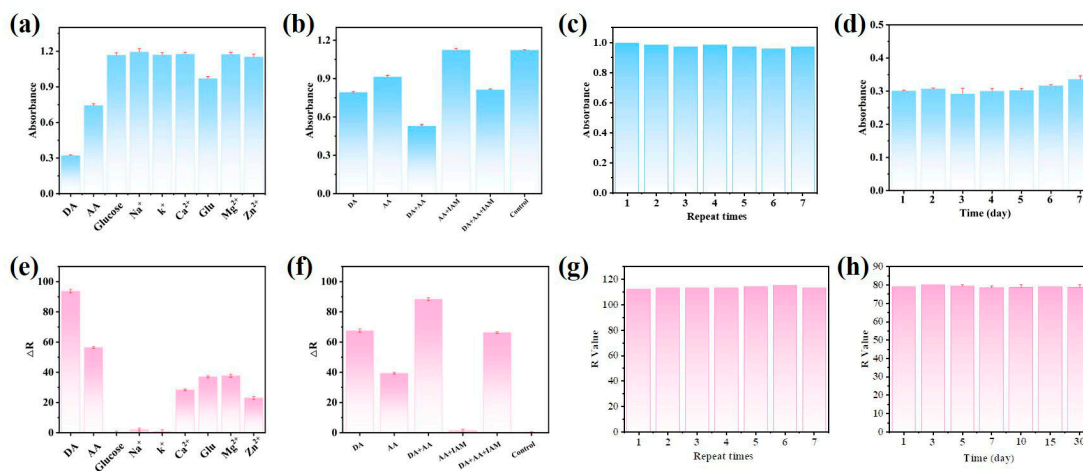


**Figure 6.** (a) Specificity of the established method for the DA of UV-vis spectra responses (other interfering compounds are present in concentrations five times (50  $\mu\text{M}$ ) greater than DA's). (e) Specificity of the established method for DA of RGB colorimetric ( $\Delta R = R - R_{\text{blank}}$ ). (b,f) The UV-vis spectra responses and RGB colorimetric values of DA, AA, and coexisting systems. The concentration of interferences is three times higher than that of DA (10  $\mu\text{M}$ ). (c,g) The repeatability of the developed method (DA = 10  $\mu\text{M}$ ). (d,h) The 30-day storage stability of the established method (DA = 50  $\mu\text{M}$  for UV-vis spectra, DA = 5  $\mu\text{M}$  for RGB colorimetric).

### 3.6. Real-Sample Analysis

The feasibility and applicability of the sensor for analyzing actual samples were further verified by testing DA added to the human serum samples of healthy volunteers and calculating the recovery rate. As shown in Table S1, the recovery rate of the standard addition by the UV-vis absorption spectrum was 94.18–105.55%, and the average recovery of the smartphone signal was 88.71–107.58%. The detection results of the two methods were compared with those of HPLC-MS/MS. After mutual fitting, the slope of the linear equation obtained by the two modes was close to 1, and the intercept was close to 0, which indicates that the two detection methods are consistent with HPLC-MS/MS and further proves that the sensor is feasible and accurate for detecting DA (Figure 7).

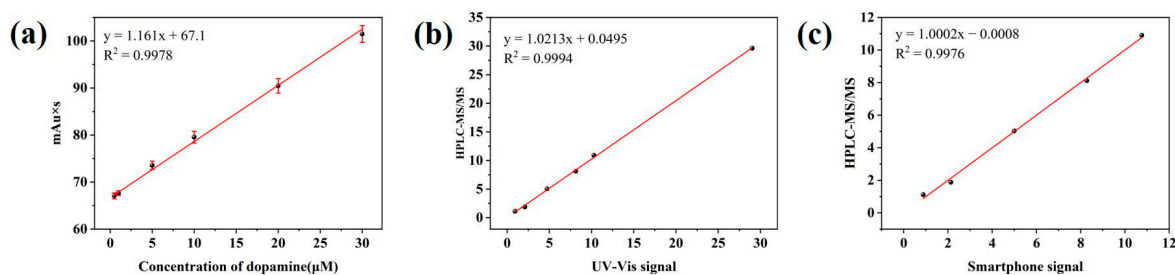


**Figure 7.** (a) Linear curve of peak area versus dopamine concentration. (b) Fitting curve of HPLC-MS/MS and UV-vis signal. (c) Fitting curve of HPLC-MS/MS and smart phone signal.

## 4. Conclusions

In this study, a rose-like CuS@PB/Pt composite was successfully fabricated. Moreover, the excellent peroxidase-like catalytic activity of the composite was observed for the first time. However, the system has economic challenges due to the use of precious metal nanomaterials. The narrow range of detection using smartphones is also a limitation. In spite of this, we developed a homogeneous colorimetric strategy for the measurement of colorimetric signals using UV-vis absorption spectroscopy that can instantly produce smartphone readouts for DA detection. The developed colorimetric sensor can be used to quantitatively analyze dopamine between 1 and 60  $\mu\text{M}$  with a detection limit of 0.28  $\mu\text{M}$ . In addition, we developed an easy-to-use portable device to aid in colorimetric detection by smartphone. The quantitative point-of-care analysis of DA is possible because of the rapid (16 min) detection time and portable smartphone readouts for detection signals. The applicability of the proposed approach for the analysis of actual sample data was demonstrated through the acceptable detection of DA in real samples by the proposed colorimetric sensor. In summary, a practical and effective colorimetric detection platform was developed for the detection of DA in human serum that will broaden the potential point-of-care applications in biotechnology and clinical diagnosis. This platform also provides a good future research direction for detecting dopamine precursors or metabolites, such as phenylalanine and tyrosine. Moreover, the potential application of novel, high-performance artificial enzyme simulations based on nanomaterials was demonstrated.

**Supplementary Materials:** The following supporting information can be downloaded at: <https://www.mdpi.com/article/10.3390/s23229029/s1>. Figure S1: (a,c) Steady-state kinetic analysis utilizing the Michaelis–Menten model of  $\text{H}_2\text{O}_2$  and TMB; (b,d) Lineweaver–Burk double-reciprocal model of  $\text{H}_2\text{O}_2$  and TMB; Figure S2. UV–Vis absorption spectra with different chromogenic reagent of the addition of DA at different concentrations ((a) ABTS; (b) (OPD)); Table S1: Determination of dopamine in human serum.

**Author Contributions:** Writing—original methodology, draft preparation, D.Y.; formal analysis, validation, H.Y. and P.F.; conceptualization, data curation, J.R.; writing—review and editing, supervision, funding acquisition, B.L. All authors have read and agreed to the published version of the manuscript.

**Funding:** This research was funded by the National Natural Science Foundation of China 17(21864007, 21605029) and the Guizhou Provincial Natural Science Foundation (Qian Ke He Ji Chu [2020] 1Y042).

**Institutional Review Board Statement:** The study was conducted in accordance with the Declaration of Helsinki and approved by the Ethics Committee of Human Medicine Experimental Ethics of Guizhou University (protocol code HMEE-GZU-2023-T011, 15 March 2023).

**Informed Consent Statement:** Informed consent was obtained from all subjects involved in the study.

**Data Availability Statement:** The data presented in this study are available on request from the corresponding author.

**Conflicts of Interest:** The authors declare no conflict of interest.

## References

1. Myslivecek, J. Dopamine and Dopamine-Related Ligands Can Bind Not Only to Dopamine Receptors. *Life* **2022**, *12*, 606. [[CrossRef](#)] [[PubMed](#)]
2. Goldman-Rakic, P.S.; Castner, S.A.; Svensson, T.H.; Siever, L.J.; Williams, G.V. Targeting the dopamine D1 receptor in schizophrenia: Insights for cognitive dysfunction. *Psychopharmacology* **2004**, *174*, 3–16. [[CrossRef](#)] [[PubMed](#)]
3. Lahlou, S.; Gabbitov, E.; Owen, L.; Shohamy, D.; Sharp, M. Preserved motor memory in Parkinson's disease. *Neuropsychologia* **2022**, *167*, 108–161. [[CrossRef](#)] [[PubMed](#)]
4. Weber, M.A.; Conlon, M.M.; Stutt, H.R.; Wendt, L.; Ten Eyck, P.; Narayanan, N.S. Quantifying the Inverted U: A Meta-Analysis of Prefrontal Dopamine, D1 Receptors, and Working Memory. *Behav. Neurosci.* **2022**, *136*, 207–218. [[CrossRef](#)]
5. Kasper, J.; Eickhoff, S.B.; Peter, J.; Dogan, I.; Wolf, R.C.; Reetz, K.; Dukart, J.; Orth, M. Functional MRI Derived Resting-State Alterations in Huntington's Disease are Associated with the Distribution of Serotonergic and Dopaminergic Neurotransmitter Systems. *Biol. Psychiatry* **2021**, *89*, S172. [[CrossRef](#)]
6. Liu, Y.; Liu, C.; Lin, Q.H.; Zhang, J.J.; Du, W.J.; Liang, J.; Sui, N. Hypothalamic Melanocortin and Mesencephalic Dopamine Systems Regulate Reward-related Behaviors in Food Intake and Drug Use. *Progress. Biochem. Biophys.* **2021**, *48*, 541–549.
7. Seeman, M.V. Philip Seeman's contributions to the story of schizophrenia. *Psychol. Med.* **2022**, *52*, 2401–2403. [[CrossRef](#)]
8. Xu, M.-S.; Fang, C.; Xu, J.; Zhang, G.-F.; Ge, L.-B. Dynamic changes of dopamine and its metabolite levels in the rat striatum after cerebral ischemia-reperfusion and electroacupuncture. *Zhen Ci Yan Jiu = Acupunct. Res.* **2009**, *34*, 230–235.
9. Pi, Z.F.; Wang, Q.Q.; Zhang, J.; Song, F.R.; Liu, Z.Q. Effect of Schisandra Fruit on Neurochemicals in Hippocampus of Diabetic Encephalopathy Rat Using Online MD-HPLC-MS/MS. *Chem. J. Chin. Univ. Chin.* **2015**, *36*, 442–448.
10. Gong, Q.-j.; Han, H.-x.; Wang, Y.-d.; Yao, C.-z.; Yang, H.-y.; Qiao, J.-l. An electrochemical sensor for dopamine detection using poly-tryptophan composited graphene on glassy carbon as the electrode. *New Carbon. Mater.* **2020**, *35*, 34–41. [[CrossRef](#)]
11. Farah, A.M.; Thema, F.T.; Dikio, E.D. Electrochemical Detection of Hydrogen Peroxide Based on Graphene Oxide/Prussian Blue Modified Glassy Carbon Electrode. *Int. J. Electrochem. Sci.* **2012**, *7*, 5069–5083. [[CrossRef](#)]
12. Qiu, H.; Yin, X.-B.; Yan, J.; Zhao, X.; Yang, X.; Wang, E. Simultaneous electrochemical and electrochemiluminescence detection for microchip and conventional capillary electrophoresis. *Electrophoresis* **2005**, *26*, 687–693. [[CrossRef](#)] [[PubMed](#)]
13. Yan, M.; Ge, S.G.; Lu, J.J.; Yu, J.H. Fluorescence Quenching Method for Determination of Dopamine Based on Double Molecular Recognition. *Chin. J. Anal. Chem.* **2011**, *39*, 1711–1715. [[CrossRef](#)]
14. Zhao, J.H.; Liu, J.X.; Tricard, S.; Wang, L.; Liang, Y.L.; Cao, L.H.; Fang, J.; Shen, W.G. Amperometric detection of hydrazine utilizing synergistic action of prussian blue @ silver nanoparticles/graphite felt modified electrode. *Electrochim. Acta* **2015**, *171*, 121–127. [[CrossRef](#)]
15. Wu, Y.; Feng, J.; Hu, G.; Zhang, E.; Yu, H.H. Colorimetric Sensors for Chemical and Biological Sensing Applications. *Sensors* **2023**, *23*, 2749. [[CrossRef](#)]
16. Liu, S.M.; Zhou, X.Y.; Lv, C.Y.; Liu, R.; Li, S.Y.; Yang, G.Y. A novel bromelain-MnO<sub>2</sub> biosensor for colorimetric determination of dopamine. *N. J. Chem.* **2021**, *45*, 92–97. [[CrossRef](#)]
17. Zhu, Z.; Wu, C.C.; Liu, H.P.; Zou, Y.; Zhang, X.L.; Kang, H.Z.; Yang, C.J.; Tan, W.H. An Aptamer Cross-Linked Hydrogel as a Colorimetric Platform for Visual Detection. *Angew. Chem.-Int. Ed.* **2010**, *49*, 1052–1056. [[CrossRef](#)]
18. Chen, J.X.; Ma, Q.; Li, M.H.; Chao, D.Y.; Huang, L.; Wu, W.W.; Fang, Y.X.; Dong, S.J. Glucose-oxidase like catalytic mechanism of noble metal nanozymes. *Nat. Commun.* **2021**, *12*, 1–12. [[CrossRef](#)]
19. Cheng, Y.Y.; Liang, L.; Ye, F.G.; Zhao, S.L. Ce-MOF with Intrinsic Haloperoxidase-Like Activity for Ratiometric Colorimetric Detection of Hydrogen Peroxide. *Biosensors* **2021**, *11*, 204. [[CrossRef](#)]
20. Sun, D.M.; Zhao, Q.; Tan, F.; Wang, X.C.; Gao, J.S. Simultaneous detection of dopamine, uric acid, and ascorbic acid using SnO<sub>2</sub> nanoparticles/multi-walled carbon nanotubes/carbon paste electrode. *Anal. Methods* **2012**, *4*, 3283–3289. [[CrossRef](#)]
21. Fan, K.L.; Xi, J.Q.; Fan, L.; Wang, P.X.; Zhu, C.H.; Tang, Y.; Xu, X.D.; Liang, M.M.; Jiang, B.; Yan, X.Y.; et al. In vivo guiding nitrogen-doped carbon nanozyme for tumor catalytic therapy. *Nat. Commun.* **2018**, *9*, 1440. [[CrossRef](#)]
22. Abdelhamid, H.N.; Sharmoukh, W. Intrinsic catalase-mimicking MOFzyme for sensitive detection of hydrogen peroxide and ferric ions. *Microchem. J.* **2021**, *163*, 105873. [[CrossRef](#)]
23. Wang, Z.; Yang, X.; Yang, J.; Jiang, Y.; He, N. Peroxidase-like activity of mesoporous silica encapsulated Pt nanoparticle and its application in colorimetric immunoassay. *Anal. Chim. Acta* **2015**, *862*, 53–63. [[CrossRef](#)] [[PubMed](#)]

24. Huang, X.; Zeng, Z.; Bao, S.; Wang, M.; Qi, X.; Fan, Z.; Zhang, H. Solution-phase epitaxial growth of noble metal nanostructures on dispersible single-layer molybdenum disulfide nanosheets. *Nat. Commun.* **2013**, *4*, 1444. [[CrossRef](#)] [[PubMed](#)]
25. Wang, Q.; Zuo, X.; Wang, X. Preparation of graphene supported Pt nanoparticles by a plasma approach and their application for methanol electro-oxidation: A comparison with chemical reduction. *Dalton Trans.* **2014**, *43*, 12961–12966. [[CrossRef](#)]
26. Wang, Y.; Zhang, X.; Luo, Z.; Huang, X.; Tan, C.; Li, H.; Zheng, B.; Li, B.; Huang, Y.; Yang, J.; et al. Liquid-phase growth of platinum nanoparticles on molybdenum trioxide nanosheets: An enhanced catalyst with intrinsic peroxidase-like catalytic activity. *Nanoscale* **2014**, *6*, 12340–12344. [[CrossRef](#)] [[PubMed](#)]
27. Wei, J.; Chen, X.; Shi, S.; Mo, S.; Zheng, N. An investigation of the mimetic enzyme activity of two-dimensional Pd-based nanostructures. *Nanoscale* **2015**, *7*, 19018–19026. [[CrossRef](#)]
28. Wu, Q.; He, L.; Jiang, Z.W.; Li, Y.; Cao, Z.M.; Huang, C.Z.; Li, Y.F. CuO nanoparticles derived from metal-organic gel with excellent electrocatalytic and peroxidase-mimicking activities for glucose and cholesterol detection. *Biosens. Bioelectron.* **2019**, *145*, 111704. [[CrossRef](#)]
29. Gao, J.J.; Liu, H.; Pang, L.Y.; Guo, K.; Li, J.Q. Biocatalyst and Colorimetric/Fluorescent Dual Biosensors of HO Constructed via Hemoglobin-Cu(PO) Organic/Inorganic Hybrid Nanoflowers. *Acs Appl. Mater. Inter.* **2018**, *10*, 30441–30450. [[CrossRef](#)]
30. Goel, S.; Chen, F.; Cai, W.B. Synthesis and Biomedical Applications of Copper Sulfide Nanoparticles: From Sensors to Theranostics. *Small* **2014**, *10*, 631–645. [[CrossRef](#)]
31. Swaidan, A.; Barras, A.; Addad, A.; Tahon, J.F.; Toufaily, J.; Hamieh, T.; Szunerits, S.; Boukherroub, R. Colorimetric sensing of dopamine in beef meat using copper sulfide encapsulated within bovine serum albumin functionalized with copper phosphate (CuS-BSA-Cu(PO)) nanoparticles. *J. Colloid. Interf. Sci.* **2021**, *582*, 732–740. [[CrossRef](#)] [[PubMed](#)]
32. Dutta, S.; Ray, C.; Mallick, S.; Sarkar, S.; Sahoo, R.; Negishi, Y.; Pal, T. A Gel-Based Approach To Design Hierarchical CuS Decorated Reduced Graphene Oxide Nanosheets for Enhanced Peroxidase-like Activity Leading to Colorimetric Detection of Dopamine. *J. Phys. Chem. C* **2015**, *119*, 23790–23800. [[CrossRef](#)]
33. Zhang, W.; Hu, S.L.; Yin, J.J.; He, W.W.; Lu, W.; Ma, M.; Gu, N.; Zhang, Y. Prussian Blue Nanoparticles as Multienzyme Mimetics and Reactive Oxygen Species Scavengers. *J. Am. Chem. Soc.* **2016**, *138*, 5860–5865. [[CrossRef](#)]
34. Zhang, W.M.; Ma, D.; Du, J.X. Prussian blue nanoparticles as peroxidase mimetics for sensitive colorimetric detection of hydrogen peroxide and glucose. *Talanta* **2014**, *120*, 362–367. [[CrossRef](#)] [[PubMed](#)]
35. Zhu, Z.Q.; Gong, L.B.; Miao, X.Y.; Chen, C.Y.; Su, S. Prussian Blue Nanoparticle Supported MoS<sub>2</sub> Nanocomposites as a Peroxidase-Like Nanozyme for Colorimetric Sensing of Dopamine. *Biosensors* **2022**, *12*, 260. [[CrossRef](#)] [[PubMed](#)]
36. Li, Y.Y.; Liu, L.; Wang, Y.G.; Ren, R.; Fan, D.W.; Wu, D.; Du, Y.; Xu, K.; Ren, X.; Wei, Q.; et al. Enzyme-free colorimetric immunoassay for procalcitonin based on MgFe<sub>2</sub>O<sub>4</sub> sacrificial probe with the Prussian blue production. *Sens. Actuators B -Chem.* **2020**, *316*, 128163. [[CrossRef](#)]
37. Liu, K.G.; Yuan, R.; Chai, Y.Q.; Tang, D.P.; An, H.Z. AuCl<sub>4</sub><sup>-</sup> and Fe<sup>3+</sup>/Fe(CN)<sub>6</sub><sup>3-</sup> ions-derivated immunosensing interface for electrochemical immunoassay of carcinoembryonic antigen in human serum. *Bioprocess. Biosyst. Eng.* **2010**, *33*, 179–185. [[CrossRef](#)]
38. Qu, J.; Chen, X.; Wang, Y.; Fan, Y.; Wang, J.; Yu, S.; Wu, M.; Hu, L. Electrochemical properties of flowerlike CuS/rGO compound material. *Ionics* **2021**, *27*, 4409–4417. [[CrossRef](#)]
39. Li, L.H.; Zhang, P.; Li, Z.Y.; Li, D.Y.; Han, B.; Tu, L.; Li, B.; Wang, Y.G.; Ren, L.; Yang, P.Y.; et al. CuS/Prussian blue core-shell nanohybrid as an electrochemical sensor for ascorbic acid detection. *Nanotechnology* **2019**, *30*, 325501. [[CrossRef](#)]
40. Shahvar, A.; Shamsaei, D.; Saraji, M. A portable smartphone-based colorimetric sensor for rapid determination of water content in ethanol. *Measurement* **2020**, *150*, 107068. [[CrossRef](#)]
41. Zhu, J.L.; Peng, X.; Nie, W.; Wang, Y.J.; Gao, J.W.; Wen, W.; Selvaraj, J.N.; Zhang, X.H.; Wang, S.F. Hollow copper sulfide nanocubes as multifunctional nanozymes for colorimetric detection of dopamine and electrochemical detection of glucose. *Biosens. Bioelectron.* **2019**, *141*, 111450. [[CrossRef](#)] [[PubMed](#)]
42. Farah, A.M.; Shooto, N.D.; Thema, F.T.; Modise, J.S.; Dikio, E.D. Fabrication of Prussian Blue/Multi-Walled Carbon Nanotubes Modified Glassy Carbon Electrode for Electrochemical Detection of Hydrogen Peroxide. *Int. J. Electrochem. Sci.* **2012**, *7*, 4302–4313. [[CrossRef](#)]

**Disclaimer/Publisher’s Note:** The statements, opinions and data contained in all publications are solely those of the individual author(s) and contributor(s) and not of MDPI and/or the editor(s). MDPI and/or the editor(s) disclaim responsibility for any injury to people or property resulting from any ideas, methods, instructions or products referred to in the content.